Available online at www.sciencedirect.com
ScienceDirect
Bioorganic & Medicinal Chemistry 15 (2007) 1556–1567
Bioorganic & Medicinal Chemistry

3D-QSAR design of novel antiepileptic sulfamides

Luciana Gavernet,[a] M. Josefina Dominguez Cabrera,[a] Luis E. Bruno-Blanch[a,*] and Guillermina L. Estiú[b,*]

[a]*Medicinal Chemistry—Department of Biological Sciences, National University of La Plata, 47 and 115, La Plata B1900BJW, Argentina*
[b]*Department of Chemistry and Biochemistry, University of Notre Dame, 251 Nieuwland Science Hall Notre Dame, IN 46556-5670, USA*

Received 5 April 2006; revised 5 June 2006; accepted 6 June 2006
Available online 8 December 2006

Abstract—A three-dimensional quantitative structure–activity relationship method, the comparative molecular field analysis (CoMFA), was applied to design new anticonvulsant symmetric sulfamides. The training set (27 structures) was comprised by traditional and new-generation anticonvulsant (AC) ligands that exhibit a potent activity in MES test. Physicochemical determinants of binding, such as steric and electrostatic properties, were mapped onto the molecular structures of the set, in order to interpret graphically the CoMFA results in terms of field contribution maps. The 3D-QSAR models demonstrate a good ability to predict the activity of the designed compounds ($r^2 = 0.967$, $q^2 = 0.756$).

1. Introduction

Two million new cases of epilepsy occur in the world every year, affecting 1–2% of the world's population.[1] Antiepileptic drugs with better safety, less toxicity, and higher efficacy in difficult-to-control patients are urgently needed, as the available ones are symptomatically effective in only 60–70% of patients.[1] Regardless of the optimal use of the available antiepileptic drugs, many patients with epilepsy fail to experience seizure control, while others do so only at the expense of significant toxic side effects.[2]

The anticonvulsant (AC) drugs have been categorized into a number of distinct classes on the basis of the molecular mechanisms through which they function.[3–6] Some of the mechanisms of AC action include: potentiation of GABA-ergic transmission,[7] blockade of voltage-gated dependent sodium channels (VGSC),[8] attenuation of excitatory neurotransmission,[8–10] and/or modulation of voltage-sensitive calcium channels.[3]

In recent years, several compounds such as felbamate (FLB), fosphenytoin sodium, gabapentin, lamotrigine, levetiracetam, oxcarbazepine (OCZ), tiagabine, topiramate (TOP), and zonisamide (ZON) have been approved as AC drugs.[11–13] Other structures, like carabersat, CGX-1007 (Conantokin-G), pregabaline, retigabine, safinamide, SPD421 (DP-VPA), remacemide, rufinamide, stiripentol, valrocemide, harkoseride, and talampanel, have been or are currently in the stage of human testing.[11–13]

Among the new drugs, some have been derived from optimization of pre-existing compounds (structure-based design). Others have been developed following a specific objective of modifying a certain stage of the mechanism (mechanism-based design) or another target, like levetiracetam with their new binding site, the synaptic vesicle protein.[11–13] The design of new anticonvulsant drugs is often hampered by the fact that the mode of action of the drugs involves more than one specific binding site and is not always linked with one specific binding site. Therefore, drug identification is partially conducted via in vivo screening tests using whole animal systems or via in vitro testing. Moreover, due to the diversity of mechanisms through which the AC action is exerted, different seizure models have been developed to evaluate the anticonvulsant activity during the research process. Among them, the maximal electroshock (MES) test and the subcutaneous pentylenetetrazole (PTZ) test are

Keywords: Anticonvulsant drugs; Sulfamides; CoMFA; Drug design.
* Corresponding authors. Tel.: +54 0221 4235333; fax: +54 0221 4223409 (L.E.B.-B.); tel./fax: +1 574 631 4007 (G.L.E.); e-mail addresses: lbb@biol.unlp.edu.ar; estiu@nd.edu

0968-0896/$ - see front matter © 2006 Elsevier Ltd. All rights reserved.
doi:10.1016/j.bmc.2006.06.010

the most widely used to characterize the anticonvulsant activity.[14] These models respond well to neuronal VGSC inhibitors and GABA-ergic compounds, respectively. In particular, those drugs that are active against the MES test, but not against the PTZ test, show a pharmacological profile similar to phenytoin (PHE), and are called phenytoin-like compounds.[2,15] The picrotoxin test (PIC), in which the chemically induced seizure is produced through the non-competitive inhibition of the GABA receptor,[7] is also extensively used, and has been applied in this investigation.

The anti-MES profile, which is mainly used to target an inhibition of the neuronal voltage-dependent Na channels, has been widely studied, and some pharmacophoric models have been developed.[16,17] The one most recently proposed is based on the comparison of 13 dissimilar structures, and combines the existence of a polar moiety (atoms 1–3, Fig. 1) and a hydrophobic chain (atoms 5–7, Fig. 1) in a well-defined spatial conformation.[18]

Other pharmacophoric models have been derived from 2D-QSAR analysis, and also revealed the importance of electronic and lipophilic regions.[19] Among them, the one developed by Unverferth et al.[16] shows three groups of different characteristics that should be present, at well-defined distances, in order for the structures to be active. These different groups involve an aryl ring, an electron donor atom, and a second donor atom which, close to the NH group, defines a hydrogen bond acceptor/donor unit. Several other model pharmacophores have been developed from the comparison of structures that belong to a given family.[17]

Nevertheless, only 3D-QSAR is capable of identifying the spatial characteristics shared by the active molecules. On the basis of this consideration, and as an additional step toward the design of AC drugs, we have applied 3D-QSAR CoMFA studies, using a set of compounds larger than the one previously used,[18] with the aim of identifying a more reliable pharmacophore for the anti-MES activity.[18]

Attending the importance of the molecular alignment for the success of the CoMFA-derived models, we have based the molecular alignment on the electrostatic and structural properties of the previously derived 3D pharmacophore shown in Figure 1.[18]

The structural variations of the compounds of the training set are reflected in variations of the CoMFA molecular fields at particular regions of the space. From their correlation with the biological activities we have designed a new class of AC structures that belong to the family of symmetric sulfamides. The design was supported by a non-classical bioisosteric replacement of the groups that contribute to the definition of the polar end. As a next step, a new CoMFA was applied to an extended set, built by the addition of the designed sulfamides to the original one.

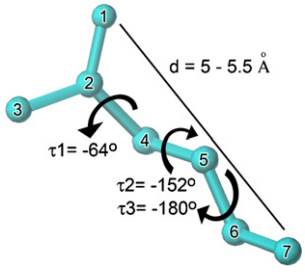

Figure 1. Structure of the pharmacophore previously proposed.[18]

Sulfamides have traditionally played a role in medicinal chemistry. They have been studied for their properties as HIV protease inhibitors,[20,21] agonists of the 5-HTID receptor,[22] active components in epinephrine analogues[23], and non-hydrolyzable components of peptide-mimetics.[24] They have also been analyzed as carbonic anhydrase inhibitors,[25–29] since almost all of the most potent inhibitors of carbonic anhydrase contain a sulfamide-related function, sulfonamide, as the anchoring group to the catalytic Zn.[30,31] Several AC drugs of clinical use, like TOP, also bear a sulfamide-related functionality. Their anticonvulsant action is probably due to CO_2 retention secondary to inhibition of the red cell and brain enzymes[29,32] but other mechanisms of action, such as blockade of sodium channels, were hypothesized/proved for some of them.[33]

This article describes the design of novel anticonvulsant-sulfamide-based ligands that would very likely keep the same anti-MES profile as the ligands of the training set from which they have been designed. The AC sulfamides have been designed from the results of a CoMFA of 27 AC drugs, which is also described here.

The presentation of the results is organized in three sections:

1. The comparative field analysis of the AC drugs that present anti-MES activity.
2. The design, synthesis, and biological evaluation of novel ligands, based on the CoMFA results.
3. The results of an extended CoMFA in which the designed structures were added to the original set.

The biological assays demonstrate the ability of the 3D-QSAR models to predict the activity of the designed compounds and the high quality of the derived model ($r^2 = 0.967$, $q^2 = 0.756$).

2. Methods

2.1. Data set and alignment

The molecular modeling and comparative molecular field evaluations were performed using SYBYL version 6.6 running on a Silicon Graphics Octane workstation.[34]

The 27 compounds selected for this study (Fig. 2) represent models for 13 structurally different classes of compounds with similar action in the experimental biological model, MES test. Classical drugs, like PHE, carbamazepine (CZ), and valpromide (VPD), are

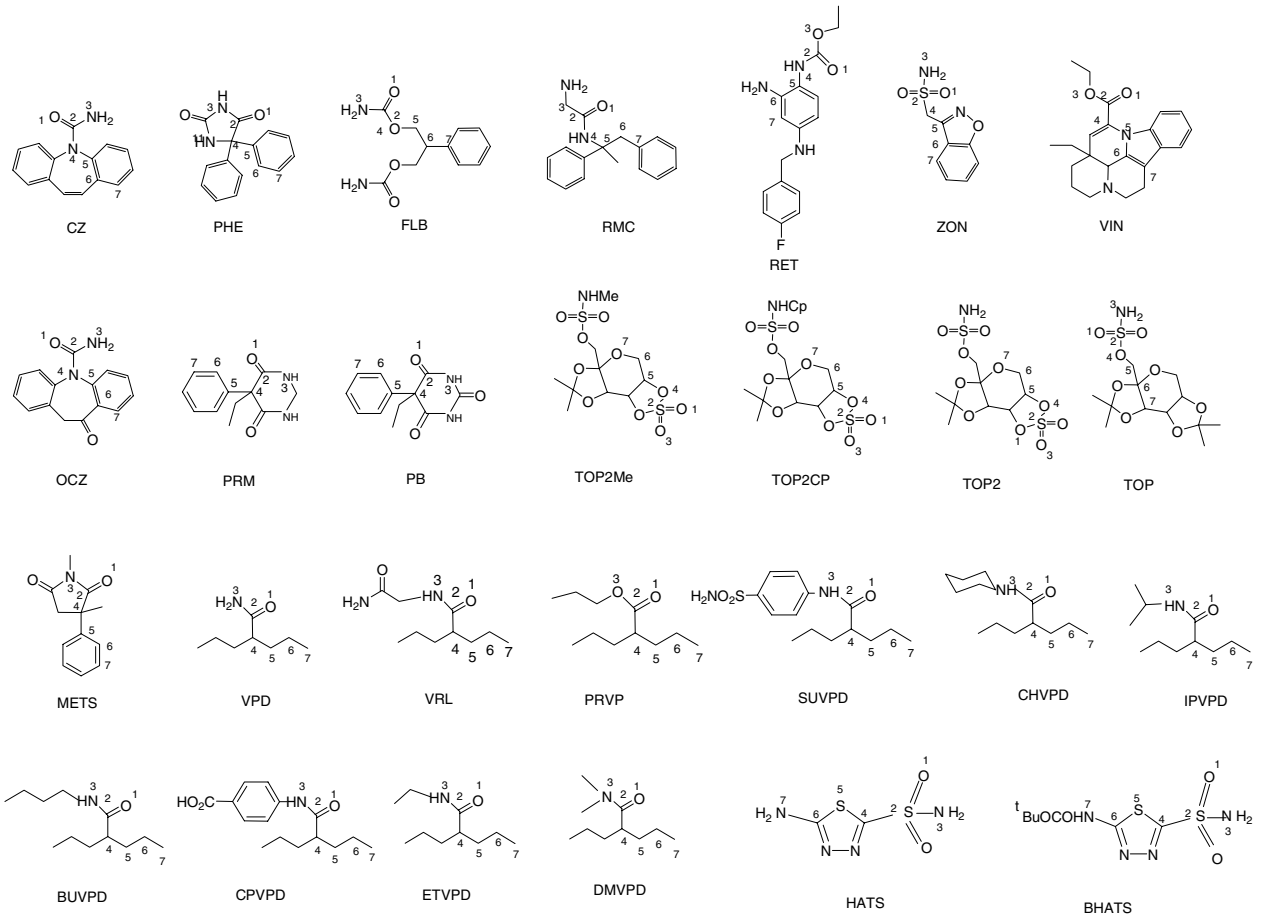

Figure 2. Structures of the AC drugs that are active in the MES test and used to define the training set. Atoms are numbered for the centers that define the pharmacophoric pattern. Other compounds included in the set and not mentioned before are: vipocentine (VIN), 2,3-*O*-isopropylidene-4,5-*O*-sulfonyl-β fructopyranose sulfamate (TOP2), *N*-methyl 2,3-*O*-isopropylidene-4,5-*O*-sulfonyl-β fructopyranose sulfamate (TOP2Me), *N*-cyclopropyl 2,3-*O*-isopropylidene-4,5-*O*-sulfonyl-β fructopyranose sulfamate (TOP2CP), valprocemide (VRL), *N*-butylvalpromide (BUVPD), *N*-cyclohexylvalpromide (CHVPD), *N*,*N*-dimethylvalpromide (DMVPD), *N*-ethylvalpromide (EtVPD), *N*-isopropylvalpromide (IPVPD), 4-(valproilamide) benzoic acid (CPVPD), *N*-(sulfonamidephenyl)valpromide (SUVPD), propyl valproate (PRVP), methsuximide (METS), phenobarbital (PB), pyrimidone (PRM), remacemide (RMC) and 5-amino-1,3,4-thiadiazole-2-sulfonamide (HATS), 5-*tert*-butoxycarbonylamino-1,3,4-thiadiazole-2-sulfonamide (B-HATS), and retigabine (RET).

included in the training set, together with new generation ones like FLB, TOP, and zonisamide (ZON). All of them have shown to block the VGSC as one of their related mechanisms of AC action.[1,13,35–37] N-Substituted valpromides and one valproate were also included, with substituents chosen so that size and polarity were varied. The synthesis and biological activity of these compounds have been already reported.[18,38] They have been designed on the basis of the consideration of the AC activity of valpromide, which supercedes valproic acid, and attending the change of the activity triggered by N-substitution. These compounds present a pharmacological profile similar to PHE.

A CoMFA study requires the coordinates of the molecules to be aligned according to reasonable bioactive conformations. To this end, we have used the conformation previously determined for the pharmacophore associated with Na-channel blocking AC drugs (Fig. 1). The atoms that define the template are numbered 1–7 in Figure 2.

In the superposition with the template, the rigid structures of the training set determine the main characteristics of the bioactive conformation. However, there are also flexible structures, bearing rotatable bonds in portions that do not overlap with the pharmacophore. In these cases, several conformations might be considered as the active one. The search for the characteristics associated with the binding of flexible molecules to receptors is a challenging task because many low-energy conformations are accessible and may coexist in equilibrium. The goal is to identify the common geometric arrangements of the moieties that are determinants of receptor recognition or activation, including all the low-energy conformations of each molecule in the analysis. Therefore, the rotatable bonds that are not part of the pharmacophore were allowed to rotate, and the set of active conformations has been defined as the one which renders the highest value of q^2 in the leave-one-out (LOO) cross-validation method included in PLS-CoMFA calculations (see PLS analysis).

As a first step, which precedes the superposition analysis, each of the 27 compounds was fully optimized by means of Density Functional Calculations (G98[39] B3LYP/6-31G**). The optimized structures have been

further fitted to the pharmacophore structural constrains using the atom fit method provided by the Sybyl software.[34] As a measure of the ability of the molecules to adopt the active conformation, the RMS values have been obtained for the superposition performed by Sybyl. In the RMS fitting the molecules were aligned by minimizing the RMS distance between corresponding atoms belonging, respectively, to the fitting molecule and to the template structure.

2.2. CoMFA 3D-QSAR model

The aligned molecules were originally placed in a three-dimensional grid of 2 Å in the x, y, and z directions. A sp^3 carbon probe atom with a charge of +1.0 and a VdW radius of 1.52 Å was used to calculate the CoMFA steric and electrostatic field descriptors. The distant dependent dielectric constant was used to treat the electrostatic terms. A default cutoff of 30 kcal/mol was used to truncate the steric field and the electrostatic field energies. CoMFA standard scaling was used.

The regression analysis has been performed by means of partial least-squares (PLS) estimation. We have initially used the leave-one-out cross-validation method in order to reduce the possibility of obtaining chance correlation and to find out the optimal number of components. In the leave-one-out technique one compound of the set was removed at a time and its activity was calculated using the QSAR model based on the remaining compounds. In this way, the internal predictive ability of the model was tested and quantified by means of the cross-validated correlation coefficient q^2. The optimal number of components was determined by the highest q^2 value and the minimum standard error of estimate SEE in the cross-validated correlation. A 2 kcal/mol energy column filter was performed to improve the signal-to-noise ratio. The steric and electrostatic field columns were then used according to the CoMFA STD default option, and the final QSAR model was calculated with PLS without cross-validation, using the optimal number of components previously determined. The quality of the model was determined by means of the conventional correlation coefficient (r^2).

2.3. Chemistry

The substituted sulfamides have been synthesized according to previously reported procedures[24,40–44] (Scheme 1 compounds **2a**–**e**), by condensation of an excess of amine with sulfuryl chloride (Scheme 1). We have found a non-favorable effect of pyridine in the reaction,[45,46] and it was not used as a reactant.

3. Results and discussion

3.1. The Comparative Field analysis of the AC drugs

3.1.1. 3D pharmacophore development. We have used a ligand-based design strategy, oriented to identify and characterize the minimal molecular requirements for AC activity, using a training set of 27 known potent anticonvulsants that are known to be active in MES test (see Fig. 2).

The compounds of the set have been used to develop a 3D-QSAR CoMFA model, which represents the three-dimensional arrangements of specific functional groups essential for activity. To this end 3D-QSAR models were constructed in the way previously explained (see data set and alignment). The molecules aligned in their active conformations are shown in Figure 3.

The analysis provided statistically reliable models of good internal predictive power. The statistical results are summarized in Table 1.

The regression coefficient (r^2) and the cross-validated r^2 (q^2) of this QSAR model based on atom fit alignment are 0.960 and 0.748, respectively, with low standard error (0.107). Based on these values, we consider that the CoMFA model presents a good quality and exhibits good predictive capability. In order to further test the reliability of the CoMFA, we have repeated the fit including valproic acid (VPA) in the set, using the ED_{50} value ($-\log ED_{50}$: -3.3), previously determined by us.[18] In this way we have broadened the range of activities considered in the analysis. The inclusion of VPA does not deviate significantly the values of the statistical descriptors ($q^2 = 0.708$; $r^2 = 0.897$, Sf = 0.672, Ef = 0.328) relative to those obtained without this compound. As VPA is known to act through several different mechanisms, we have chosen to analyze the results of the previous CoMFA (Table 1). Nevertheless, the stability of the q^2 value after the inclusion of VPA reinforces the significance of our results.

Table 2 lists the measured and predicted activities (columns 2 and 5, respectively), as well as the RMS values calculated with the compounds of the training set. The values of residuals estimated from the comparison between predicted and experimental values (column 6) are also shown. These values are lower than 0.25 and only in eight cases (30%) are larger than ±0.1.

3.1.2. Visualization of the QSAR results. The results obtained were graphically interpreted in terms of field

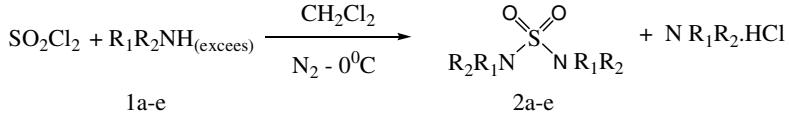

1a-e 2a-e

2: a, R_1 = ^{n}Bu, R_2= H; b, R_1 = Cyclohexyl, R_2= H; c, R_1 =Benzyl R_2= H; d, R_1 = Cyclopropyl, R_2= H; e, R_1R_2= Morpholine

Scheme 1. Synthetic route for sulfamides.

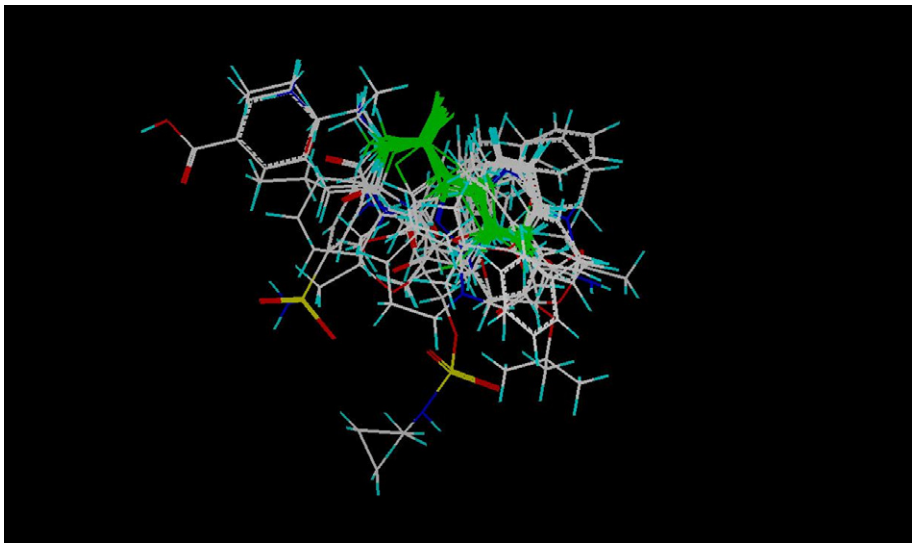

Figure 3. Molecules aligned in the conformation used in CoMFA. The atoms used for superimposition are shown in green.

Table 1. Statistical results using CoMFA

	Statistical results
ONC[a]	4
q^{2}[b]	0.748
r^{2}[c]	0.960
SEE[d]	0.107
Sf[e]	0.672
Ef[f]	0.328
Res[g]	0.079

[a] ONC, optimum number of components.
[b] q^2, cross-validated r^2.
[c] r^2, non-cross-validated r^2.
[d] SEE, standard error estimate.
[e] SF, steric field.
[f] Ef, electrostatic field.
[g] Res, average of residuals.

contribution maps, which are shown in Figure 4, with CZ as the reference molecule.

The contour maps have permitted an understanding of the steric and electrostatic requirements for ligand binding. Physicochemical determinants of binding, such as steric and electrostatic properties, have different contributions to the CoMFA model. As reported, the steric contribution (Sf, Table 1) is more than two times larger than the electrostatic one (Ef Table 1). This is indicative of a larger influence of the steric effect in modulating the AC activity.

The alignment method used in this study was based on the fitting of the atoms that define the pharmacophoric pattern. After their superposition, they have almost the same coordinates in the CoMFA 3D space grid. Besides, their electronic characteristics are similar, since the pharmacophore derivation has been also based on the comparison of the charges on the corresponding atoms.[18] Because of this, the contributions of the pharmacophore atoms to CoMFA descriptors are similar, and the structural variations in the training set that give rise to variations in the molecular fields at particular regions of the space are mainly related to portions of the molecules that are not included in the pharmacophore.

From the CoMFA correlation of the aligned structures with their activities, and from the inspection of the 'pharmacophore side chains' a new requirement for the AC activity has been derived on the basis of the following considerations.

- In the steric contour (Fig. 4a), two regions have been identified (in green), where the addition of bulky groups may increase activity. Special attention has been given to the green region close to the polar end of the pharmacophore (a-1). This region is close to atom 3 in Figure 1. Thence, an increase in the activity can be attained through the addition of bulky substituents to the polar moiety of the pharmacophore. The characteristics of the group are partially dictated by the presence of a yellow region, which exerts a negative effect on the activity. The optimum orientation of the substituent, which minimizes interactions with the yellow region, is associated with a value of $\tau 4$ close to 0° (Fig. 4). Among the compounds of the set, the highest activity is attained by molecules like PB, PHE, and PRM, which have a bulky substituent in the orientation required. These compounds have a value of $\tau 4$ close to 0, which is fixed by a rigid portion. The green region a-2 may be considered an extension of the non-polar portion in the pharmacophore, attending the way it is positioned relative to the non-polar end. In this way, whereas the size of the non-polar part shown in Figure 1 is the minimum one required for activity, a larger size may increase the AC potency.
- The yellow contours identify regions where the addition of bulky groups may decrease activity (region a-3). They are located near the polar end of the pharmacophore, opposite to the green region, as it was previously discussed. The analysis of the green and yellow regions provides an explanation to the low activity of the METS molecule when compared to

Table 2. Biological data measured and predicted

Compound	ED_{50}[a]	RMS fit	$-\log ED_{50}$	CoMFA		Extended CoMFA	
				$-\log ED_{50}$ predicted	Residuals	$-\log ED_{50}$ predicted	Residuals
CZ	37	0.000	−1.57	−1.64	0.07	−1.64	0.07
PHE	38	0.104	−1.58	−1.72	0.14	−1.74	0.16
FLB	210	0.213	−2.32	−2.22	−0.10	−2.29	−0.03
RMC	292	0.118	−2.47	−2.47	0.00	−2.50	−0.03
RET	30.67	0.094	−1.49	−1.53	0.04	−1.49	0.00
ZON	92	0.499	−1.96	−1.89	−0.07	−1.84	0.12
VIN	77	0.706	−1.89	−1.91	0.02	−1.96	−0.07
OCZ	79	0.142	−1.90	−1.73	−0.17	−1.77	−0.13
PRM	52.3	0.200	−1.72	−1.83	0.11	−1.78	0.06
PB	93.9	0.308	−1.97	−1.89	−0.08	−1.89	−0.08
TOP2ME	22.3	0.846	−1.35	−1.36	0.01	−1.35	−0.00
TOP2CP	20.4	0.846	−1.31	−1.33	0.02	−1.33	−0.02
TOP2	19.8	0.846	−1.30	−1.38	0.08	−1.36	0.06
TOP	112	0.276	−2.05	−1.98	−0.07	−1.98	−0.07
METS	377.5	0.062	−2.58	−2.33	−0.25	−2.37	−0.21
VPD	353	0.222	−2.55	−2.49	−0.06	−2.57	−0.02
VRL	759.5	0.091	−2.88	−2.93	0.05	−2.92	0.04
PRVP	96	0.089	−1.98	−2.07	0.09	−2.04	0.06
SUVPD	53	0.088	−1.72	−1.64	−0.08	−1.72	−0.00
CHVPD	61	0.088	−1.79	−1.95	0.16	−1.90	0.11
IPVPD	384	0.088	−2.58	−2.69	0.11	−2.67	0.09
BUVPD	487	0.088	−2.69	−2.74	0.05	−2.69	0.00
CPVPD	1225	0.088	−3.09	−3.09	0.00	−3.09	0.00
ETVPD	200	0.087	−2.30	−2.17	−0.13	−2.18	−0.12
DMVPD	347	0.088	−2.54	−2.65	0.11	−2.65	0.11
HATS	90	0.493	−1.95	−1.94	−0.01	−1.88	0.07
B-HATS	74	0.493	−1.87	−1.83	−0.04	−1.81	0.06
DBS	295	0.296	−2.47	—	—	−2.40	0.07
DCHS	251	0.601	−2.18	—	—	−2.29	0.11
DBZS	238	0.293	−2.38	—	—	−2.30	0.08

Residuals and RMS fit values are also given.

[a] Experimental activity ED_{50}: median effective dose (ED50, μmol/kg) measured in the MES test (from the literature).[2,37,38,47–52]

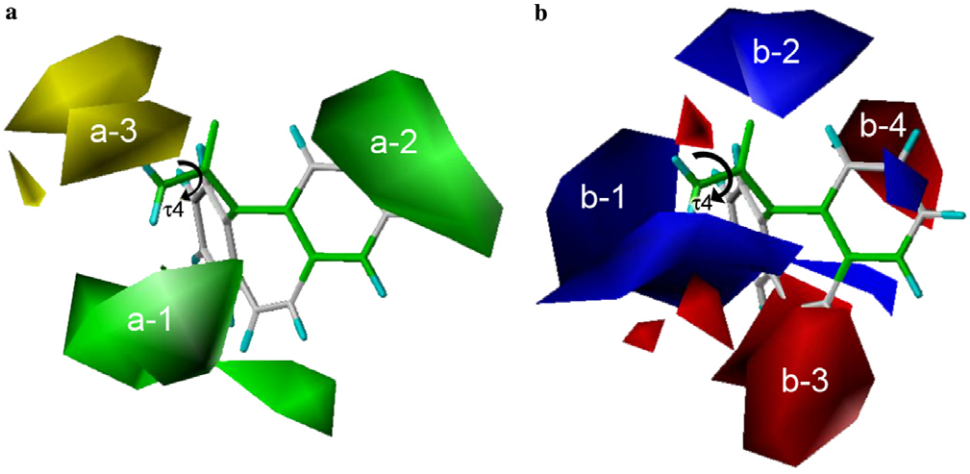

Figure 4. Electrostatic and Steric Fields of the CoMFA contour map with CZ molecule as reference. The pharmacophoric pattern is shown in green for CZ. (a) Green contours indicate the regions where the addition of bulky groups may increase activity. Yellow contours indicate the regions where the addition of bulky groups may decrease activity. (b) Blue contours indicate regions where positive groups may increase the activity. Red contours indicate regions where negative groups may increase activity. The most important regions are identified by numbers.

PB, PHE, and PRM. Whereas PB, PHE, and PRM bear substituents in the green region that define a rigid structure and a value of $\tau 4$ close to 0, the N-methyl substituent of METS is located in the yellow zone. This observation can be used to justify its lower activity.

- Several other compounds bear bulky moieties near the polar end. Nevertheless, in most of the cases $\tau 4$ is not fixed but defined by a rotatable bond. For these cases, the influence of the green and yellow regions on the AC was examined in detail through the evaluation of the cross-validated correlation coefficient (q^2). A good correlation was obtained for values of $\tau 4$ close to 0° in the most active compounds (ED_{50} lower than 200 mmol/kg), and close to 180° in less active ones (ED_{50} greater than 200 mmol/kg).

The previous observations led us to conclude that the differences in the activities are originated in the presence (or absence) of substituents occupying the green region a1 (see Fig. 4a). The optimum size and directionality of this substitution is determined by the positive and negative influences of the green and yellow regions on the activity. The directionality of the subtituent can be defined through the value of the torsion angle $\tau 4$, for which an optimum value of zero degree has been derived. The size can be defined averaging the distance from atom 2 of the pharmacophore (Fig. 1) to the atom of the substituent that, being part of the green region, is farther from it. From this average, which extends over the active compounds, a distance between 4 and 7 Å can be estimated, corresponding to an approximate size of 3 Å for the substituent. From this analysis, we conclude that the consideration of an additional requirement would certainly help to optimize the AC activity of a given compound. This requirement is associated with the presence of a bulky substituent attached to the polar moiety, oriented in a way that defines values of $\tau 4$ close to 0° (Fig. 5).

The new requirement allows us to explain the fact that several TOP derivatives have higher activities than TOP itself. In this subset of compounds, the consideration of the sulfamate/sulfate function as the polar end renders the highest value of q^2 in the leave-one-out cross-validation method. In this way, the spatial orientation of the TOP derivatives (Fig. 6) places the methyl groups of the 2,3-*O*-isopropylidene-4,5-*O*-sulfonyl-β fructopyranose in the green portion (a-1, Fig. 4). In TOP, the methyl groups are not able to accommodate in this position.

The electronic contour map shown in Figure 4b does not allow an easy interpretation. There are several red zones

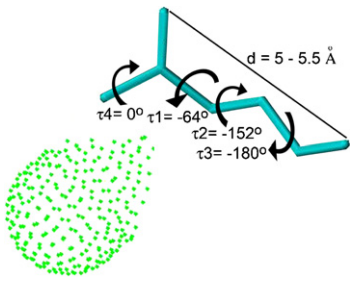

Figure 5. Structure of the new proposed pharmacophore. The additional requirement described as a bulky region is shown in green and its preferred orientation defined through $\tau 4$.

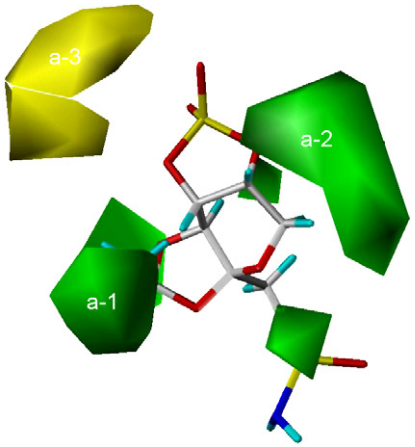

Figure 6. Spatial orientation of TOP2 relative to the steric contours derived from CoMFA.

(like b3 and b4) that indicate regions where negative groups may increase activity and blue zones where positive groups may raise the activity. The position of the blue zones (b1, b2) perfectly matches those of the negative end of the pharmacophore (atoms 1 and 3, Fig. 1). Moreover, the presence of a positive charge near these blue regions (b1, b2), or a negative charge near the red zones (b3, b4), may point to key features to be considered in the further design of AC ligands.

3.2. The design, synthesis, and biological evaluation of novel ligands, based on the CoMFA results

3.2.1. Rational design and bioisosteric substitution. The results of the CoMFA model were used to design new active prototypes. The design was mainly based on the information derived from the analysis of the steric properties, which seem to more largely determine the AC activity (Table 1).

As the template used for the alignment (Fig. 5) was a 'through space' 3D pharmacophore, rather than a 'through bonds' 2D pharmacophore, compounds with entirely different molecular scaffolds may be searched to comply with it. With the spatial orientation of the bulky portions defined, bioisoteric functional group information has been used to design a new polar moiety. In order to do this, we have analyzed the atoms that define the polar moiety of the pharmacophore (numbered 1–3 in Fig. 1) and the bioisosteric replacement of a group by sulfoxide or sulfone functionality.[53–55]

Following this line, we have designed five N-alkyl disubstituted symmetric sulfamides. The structures, (shown in Fig. 7) were prepared before by other authors.[24,40–44] We have synthesized them according to the literature and evaluated their AC activity in our laboratory for the first time.

The set of sulfamides comprises two compounds (DBS, DBZS) that are able to adopt the conformation defined by the new proposed pharmacophore (Fig. 5). Their non-polar portions can acquire the values

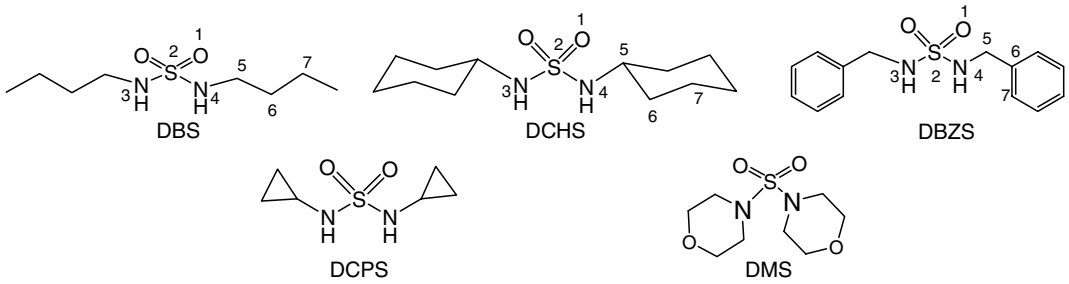

Figure 7. Structures of the sulfamides synthesized and evaluated. Atoms are numbered for the centers that define the pharmacophoric pattern in active sulfamides.

determined for the torsion angles. The other three structures of the set are rigid in their hydrophobic portion (DCPS, DMS, and DCHS). Due to the lack of rotation of its hydrocarbon chain, DCPS is unable to fit the structural constrains of the pharmacophore hydrophobic chain (atoms 5–7, Fig. 5) and can be predicted to be inactive.

3.2.2. Pharmacology. The sulfamides were tested for (AC) activity by their ability to suppress experimentally induced convulsions in laboratory animals. The tests used were the MES test, related to electrical induction; and the PTZ and PIC tests, which generate the seizure by chemical induction. The RotoRod test was used to determine the neurotoxic effects. The results obtained are listed in Table 3. The AC activity was expressed as ED_{50}, which measures the dose that is effective in 50% of the tested animals.

MES tests, PTZ tests, and PIC tests were performed following the standard procedures provided by the antiepileptic drug development program developed by the National Institute of Health.[50]

According to our prediction, DBS, DCHS, and DBZS are active in the MES tests, whereas DMS and DCPS are inactive at the doses evaluated. This behavior is interpreted in the next section in light of the CoMFA results.

Details for the evaluation of anticonvulsant activity and determination of Median Effective Dose are given in the experimental section.

3.3. Results of extended CoMFA

CoMFA was applied to an extended set, built by the addition of the active sulfamides to the original set (Fig. 2). The same alignment procedure, CoMFA parameters, and PLS analysis previously described have been followed. Atoms numbered 1–7 in the Figure 7 were used to fit the sulfamides with the pharmacophore template. Table 2 shows the RMS values obtained from the superimposition of the sulfamides with the pharmacophoric pattern, together with the biological data used for CoMFA study.

The RMS values of Table 2 are in agreement with the fact that DBS and DBZS present a bulky portion capable of adopting the pharmacophore conformation (Fig. 8), and responsible for the steric effect. This portion is absent in the inactive molecules (DCPS and DMS). The higher RMS value of DCHS is originated in the rigidity of the cyclic portion that defines the non-polar end of the pharmacophore. This rigidity precludes a perfect overlapping of the bulky moiety, but allows it to fill the same region of the space, generating similar steric effect.

For the electrostatic effect, two different descriptions have been compared, which are based on Gasteiger–

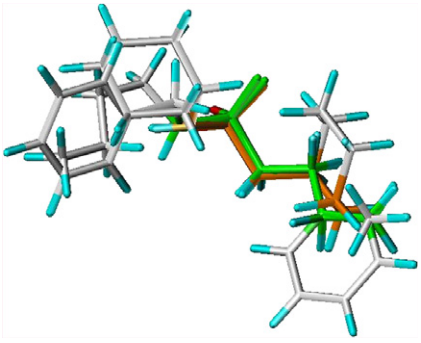

Figure 8. Superposition of DCHS, DBS, and DBZS with the pharmacophore conformation. The pharmacophoric portion is shown in orange for DCHS and in green for DBS and DBZS.

Table 3. Activity values (ED_{50}, μmol/kg) and time of peak effect (TPE) determined (mice) for the sulfamide derivatives designed in this research work

Compound	ED_{50} MES test (μmol/kg)	TPE MES test	ED_{50} PTZ test (μmol/kg)	ED_{50} PIC test (μmol/kg)
DBS	295 (246–355)	2 h	Inactive	Inactive
DCHS	151 (91–253)	30 min	Inactive	Not tested[a]
DBZS	238 (153–371)	2 h	Inactive	Inactive
DCPS	Inactive	—	Inactive	Inactive
DMS	Inactive	—	Inactive	Inactive

Compounds are defined as inactive when they are not effective at the doses evaluated (lower than 290 μmol/kg).
[a] Due to the low solubility of the drug.

Table 4. Statistical results using CoMFA for both models

Method	Model 1	Model 2
Charge	Gasteiger–Huckel	Merz–Kollman
ONC[a]	3	3
q^{2}[b]	0.756	0.681
r^{2}[c]	0.967	0.941
SEE[d]	0.093	0.121
Sf[e]	0.663	0.595
Ef[f]	0.337	0.405
Res[g]	0.068	0.085

[a] ONC, optimum number of components.
[b] q^2, cross-validated r^2.
[c] r^2, non-cross-validated r^2.
[d] SEE, standard error estimate.
[e] SF, steric field.
[f] Ef, electrostatic field.
[g] Res, average of residuals.

Huckel charges (implemented in Sybyl-model 1) and on a Merz–Kollman approximation (G98-model 2), respectively. The statistical results of the CoMFA are summarized in Table 4, showing no significant difference between the two models.

Both analyses render statistically reliable models of good predictive power. Good cross-validated q^2, together with acceptable r^2 values, confirm the dependence between the molecular descriptors that we have chosen (electrostatic and steric fields) and the biological activities of the molecules.

The statistical parameters obtained from the extended CoMFA study are comparable with those derived from the original CoMFA. This result is to be expected, since the sulfamides included in the new set have been designed on the basis of the results of the first analysis.

The contribution of the steric field was higher than the electrostatic field in both cases (approximately 60–70% of the total). The activities measured and estimated from the use of model 1 are reported in Table 2 (columns 4 and 7, respectively) together with the values of residuals (column 8), as another demonstration of the good predictability of this model. The residual values are lower than 0.21 and the number of residuals which are larger than ±0.1 in 8 (27% of the total).

The contour plot of the CoMFA field for model 1 is shown in Figure 9. It closely resembles the one obtained with the original set (Fig. 3).

The electrostatic map in Figure 9b shows two main regions where the positive potential is favorable for AC activity (colored in blue) and two main regions where the model favors the negative charge (in red). They show a good correspondence with the areas obtained in the original set (Fig. 4b). In terms of steric fields (Fig. 9a), the similarity is even larger, as both models result in the same green and yellow regions.

4. Conclusions

A 3D-QSAR model has been developed for a series of chemically diverse AC drugs, related by a common pharmacological profile: the drugs are active against the MES test. Moreover, most of them are inactive against PTZ test (phenytoin-like compounds). The model points to a steric effect as higher determinant of the activity.

The CoMFA, applied to a training set of 27 diverse structures, validates the pharmacophore previously proposed, which is associated with polar and lipophilic regions. In addition, it led to the definition of a new requirement: one or more substituents capable of filling the green region a1 (Fig. 4). The substituents can be of the size of the green portion or larger, but have to avoid interactions with the yellow portion. The required orientation can be defined by a torsion angle (τ4, Fig. 5) close to 0°.

In order to test the predictive power of the new pharmacophore, new active compounds have been designed, synthesized, and evaluated. The design was largely based on a bioisosteric substitution of the amide moiety by a sulfamide functionality. We have chosen this substitution on the consideration that amide groups define

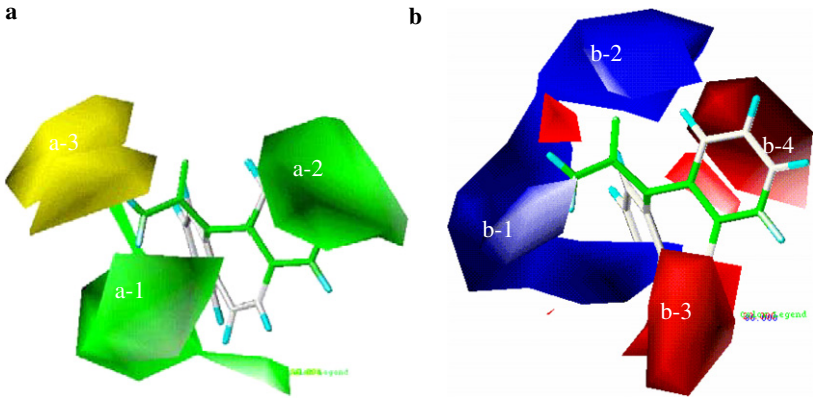

Figure 9. Electrostatic and steric fields of the CoMFA contour maps obtained with the extended set, using the CZ molecule as reference. The pharmacophore is shown in green. (a) Green contours indicate the regions where the addition of bulky groups may increase activity. Yellow contours indicate the regions where the addition of bulky groups may decrease activity. (b) Blue contours indicate regions where positive groups may increase the activity. Red contours indicate regions where negative groups may increase activity.

the polar portion in a large number of compounds of the set. The new compounds perfectly fit in the CoMFA model. The active sulfamides show the pharmacological profile characteristic of phenytoin-like compounds. They are inactive against the PIC and PTZ tests at the doses evaluated (lower than 290 μmol/kg). Their anti-MES activities are closer to those of classical and new-generation AC drugs (see Table 1), with ED_{50} values close to those determined for RMC and ETVPD; and lower than those obtained for METS, VRL, VPD, IPVPD, BUVPD, CPVPD, and DMVPD. According to their anti-MES activity, the active sulfamides have been classified as class 1 anticonvulsants[17] (anticonvulsant activity at 100 mg/Kg or less), the most potent class of antiepileptic drugs.

The active *N*,*N*′-dialkylsulfamides define new active prototypes. Compounds bearing this functionality are the focus of our present research. A rational modification of these structurally simple structures can lead to new AC drugs of optimized potency, attained by a balanced combination of polar and non-polar groups in the active structure.

5. Experimental

5.1. Chemistry

The sulfamides shown in Scheme 1 were synthesized according to the literature,[24,40–44] in the way previously described in Section 2. The compounds were identified and characterized by elemental analyses, ^1H, ^{13}C NMR,and IR spectroscopy. The equipmentsused were a Carlo Erba EA1108 apparatus, a Bruker AC-200 spectrometer with tetramethylsilane as an internal standard, and a Bruker IFS 66 spectrometer.

5.1.1. *N*,*N*′-Dibutylsulfamide (2a). This compound was prepared according to the general procedure, using *n*-butylamine (5.70 mL, 57.6 mmol, 6 equiv) in CH_2Cl_2 (5 mL) and SO_2Cl_2 (0.77 ml, 9.6 mmol, 1 equiv) in CH_2Cl_2 (5 mL). Purification of the resulting oily colorless residue through column chromatography (SiO_2, dichloromethane) affords the sulfamide **2a** (1.98 g, 75% yield) as a white solid. Mp 127–127.5 °C (CH_2Cl_2); (described 126.5 °C,); R_f: 0.36 (SiO_2, CH_2Cl_2). IR (KBr): 3286 (NH), 1313, 1142 (SO_2). ^1H NMR ($CDCl_3$): 4.55 (br t, J = 6.0 Hz, 2H: NH), 3.04 (m, 4H: α-CH_2) 1.52 (m, 4H: β-CH_2), 1.37 (m, 4H: γ-CH_2), 0.93 (t, J = 7.1 Hz, 6H: CH_3). ^{13}C NMR ($CDCl_3$): 43.10 (α-C), 31.80 (β-C), 20.11 (γ-C), 13.89 (CH_3). Anal. Calcd for $C_8H_{20}N_2O_2S$: C, 46.6; H, 8.8; N, 13.6; S, 15.5. Found: C, 46.4; H, 9.1; N, 13.2; S, 15.4.

5.1.2. *N*,*N*′-Dicyclohexylsulfamide (2b). This compound was prepared according to the general procedure, using a solution of cyclohexylamine (5.25 mL, 46.2 mmol, 6 equiv) in CH_2Cl_2 (5 mL) and SO_2Cl_2 (0.62 ml, 7.7 mmol, 1 equiv) in CH_2Cl_2 (5 mL). After 20 h of reaction, the resulting solution was filtered, and the organic layer was washed with 5% HCl (2×), brine (2×), and dried (SO_4Na_2). The solution was filtered, concentrated under reduced pressure to leave a white solid (1.68 g). Crystallization with CH_2Cl_2 afforded (622 mg, 31% yield) of sulfamide **2b** as a white solid. Mp 154–155 °C (CH_2Cl_2) (described 151–153 °C). R_f: 0.38 (SiO_2, CH_2Cl_2). IR (KBr): 3283 (NH), 1337, 1138 (SO_2). ^1H NMR ($CDCl_3$): 4.35 (d, J = 7.6 Hz, 2H: NH), 3.16 (m, 2H: CH), 2.01–1.12 (m, 20H: 2 $(CH_2)_5$). ^{13}C NMR ($CDCl_3$): 52.63 (α-C), 34.01 (β-C), 25.27 (δ-C), 24.78 (γ-C). Anal. Calcd for $C_{12}H_{24}N_2O_2S$: C, 55.8; H, 8.6; N, 10.8; S, 12.4. Found: C, 55.4; H, 8.9; N, 10.5; S, 12.4.

5.1.3. *N*,*N*′-Dibenzylsulfamide (2c). This compound was prepared according to the general procedure, using a solution of benzylsulamine (4.7 mL, 43.2 mmol, 6 equiv) in CH_2Cl_2 (5 mL) and SO_2Cl_2 (0.58 ml, 7.2 mmol, 1 equiv) in CH_2Cl_2 (5 ml). After 22 h of reaction, the resulting solution was filtered, and the organic layer was washed with 3% HCl (2×), brine (2×), and dried (SO_4Na_2). The solution was filtered, concentrated under reduced pressure to leave a white solid (804 mg). Crystallization with MeOH afforded (816 mg, 36% yield) of sulfamide **2c** as a white solid. Mp 181–183 °C (MeOH); (described 180–182 °C.). R_f: 0.36 (SiO_2, CH_2Cl_2). IR (KBr): 3277 (NH), 3088, 3065, 3033 (CH-Ar), 1321, 1148 (SO_2). ^1H NMR (DMSO-d_6): 7.47 (br s, 2H: NH), 7.31 (m, 10H: Ar-H), 4.01 (s, 4H: CH_2). ^{13}C NMR (DMSO-d_6): 138.36 (C^1-Ar), 128.25, 127.72, 127.06 ($C^{2,3,4}$-Ar), 45.81 (CH_2). Anal. Calcd for $C_{14}H_{16}N_2O_2S$: C, 61.3; H, 5.1; N, 10.2; S, 11.7. Found: C, 60.9; H, 5.5; N, 9.9; S, 11.9.

5.1.4. *N*,*N*′-Dicyclopropilsulfamide (2d). This compound was prepared according to the general procedure, using a solution of cyclopropylamine (4.84 mL, 68.4 mmol, 6 equiv) in CH_2Cl_2 (5 mL) and SO_2Cl_2 (0.91 ml, 11.4 mmol, 1 equiv) in CH_2Cl_2 (5 mL). After 30 h of reaction, CH_2Cl_2 (20 mL) was added, and the solution was washed with 3% HCl (2×), brine (2×) and dried (SO_4Na_2). The solution was filtered, concentrated under reduced pressure to leave a white solid (1.7 g). Crystallization with hexane/CH_2Cl_2 afforded (965 mg, 48% yield) of sulfamide **2d** as a white solid. Mp 147–149 °C (Hexane/CH_2Cl_2). R_f: 0.36 (SiO_2, CH_2Cl_2). IR (KBr): 3271 (NH),1316, 1142 (SO_2). ^1H NMR ($CDCl_3$): 5.01 (s, 2H: NH), 1.98 (m, 2H: α-CH), 0.71 (m, 8H: β-CH_2). ^{13}C NMR ($CDCl_3$): 24.15 (α-C), 6.02 (β-C). Anal. Calcd for $C_6H_{12}N_2O_2S$: C, 41.4; H, 5.8; N,16.1; S,18.4. Found: C, 41.1; H, 6.2; N, 15.8; S, 18.2.

5.1.5. *N*,*N*′-Sulfonil bis tetrahydro-1,4-oxazine (2e). This compound was prepared according to the general procedure, using a solution of morpholine (4.2 ml, 50.8 mmol, 6 equiv) in CH_2Cl_2 (5 mL) and SO_2Cl_2 (0.68 ml, 8.5 mmol, 1 equiv) in CH_2Cl_2 (5 mL). After 17 h of reaction, the solvent was concentrated under reduced pressure to leave a crude yellow oil. Column chromatography (SiO_2, CH_2Cl_2) afforded 1.66 g of a solid. Crystallization with Cl_4C afforded (1.47 g, 73% yield) of sulfamide **5a** as a white solid. Mp 141–142.5 °C (Cl_4C). R_f: 0.72 (SiO_2, AcOEt). IR (KBr): 1334, 1131 (SO_2). ^1H NMR ($CDCl_3$): 3.73 (t, J = 4.9 Hz, 8H: CH_2–O), 3.25 (t, J = 4.9 Hz, 8H: CH_2N). ^{13}C NMR ($CDCl_3$): 66.32 (C–O), 46.55 (C–N). Anal. Calcd for

$C_8H_{16}N_2O_4S$: C, 40.7; H, 6.8; N, 11.9; S, 13.6. Found: C, 40.9; H, 6.6; N, 12.3; S, 13.3.

5.2. Biological data

The evaluation of the anticonvulsant activity followed the Anticonvulsant Drug Development (ADD) Program of the National Institute of Health.[50] Adult male and female albino mice (18–25 g) were used as experimental animals. Animals of the same age and weight have been selected, in order to minimize biological variability. The animals were maintained on a 12-h light/dark cycle and allowed free access to food and water, except during the time they were removed from their cages for testing. The test substance was administered in 30% polyethylene glycol 400 (PEG) and 10% water. The drugs were administered intraperitoneally (ip) in mice in a volume of 0.01 ml/g body weight.

5.3. Determination of median effective dose (ED_{50})

All quantitative studies were conducted at the previously determined time of peak effect (TPE). The ED_{50} was determined by treating groups of six albino mice. Different doses were used for each drug at TPE. The method of Litchfield and Wilcoxon[56] was used to compute the ED_{50} and 95% confidence intervals.

The AC activity of valproic acid, valproate, valpromide, and their derivatives was determined in the way previously reported.[18,37] All the other biological data were taken from the literature[2,37,38,47–52] for assays where the drugs were administered intraperitoneally.

Acknowledgments

L. E. Bruno-Blanch is a member of the Facultad de Ciencias Exactas, Universidad Nacional de La Plata; L. Gavernet is a fellowship holder of Consejo Nacional de Investigaciones Científicas y Técnicas de la República Argentina (CONICET). J. Domínguez is a fellowship holder of Agencia de Promoción Científica y Tecnológica. This research was supported in part through grants from Agencia de Promoción Científica y Tecnológica (PICT 06-11985/2004), CONICET, and Universidad Nacional de La Plata, Argentina.

References and notes

1. White, H. S. *Epilepsia* **2003**, *44*(Suppl. 7), 2.
2. Vamecq, J.; Bac, P.; Herrenknecht, C.; Maurois, P.; Delcourt, P.; Stables, J. *J. Med. Chem.* **2000**, *43*, 1311.
3. Macdonald, R. L.; Kelly, K. M. *Epilepsia* **1995**, *36*, S2.
4. Sills, G. J.; Brodie, M. J. *Epileptic Disord.* **2001**, *3*, 165.
5. Faingold, C. L. In *Drugs for Control of Epilepsy: Actions of Neuronal Networks Involved in Seizure Disorders*; Faingold, C. L., Fromm, G. H., Eds.; CRC Press: Boca Raton, FL, 1992; pp 57–68.
6. Meldrum, B. S. *Epilepsia* **1996**, *37*, S4.
7. Sarkisian Mathew, R. *Epilepsy & Behavior 2,* **2001**, 201.
8. Foster, A. C.; Fagg, G. E. *Brain Res. Rev.* **1984**, *7*, 103.
9. Meldrum, B. S. *Epilepsy Res.* **1992**, *12*, 189.
10. Rogawski, M. A.; Porter, R. J. *Pharmacol. Rev.* **1990**, *42*, 223.
11. Bialer, M.; Johannessen, S. I.; Kupferberg, H. J.; Levy, R. H.; Perucca, E.; Tomson, T. *Epilepsy Res.* **2004**, *61*, 1.
12. Bialer, M.; Johannessen, S. I.; Kupferberg, H. J.; Levy, R. H.; Loiseau, R. H.; Perucca, E. *Epilepsy Res.* **2002**, *51*, 31.
13. Bialer, M.; Johannessen, S. I.; Kupferberg, H. J.; Levy, R. H.; Loiseau, R. H.; Perucca, E. *Epilepsy Res.* **2001**, *43*, 11.
14. Loscher, W.; Schmidt, D. *Epilepsy Res.* **1994**, *17*, 95.
15. Anger, T.; Madge, D.; Mulla, M.; Riddall, D. *J. Med. Chem.* **2001**, *44*, 115.
16. Unverferth, K.; Engel, J.; Höfgen, N.; Rostock, A.; Günther, R.; Lankau, H.-J.; Menzer, M.; Rolfs, A.; Liebscher, J.; Müler, B.; Hofmann, H.-J. *J. Med. Chem.* **1998**, *41*, 63.
17. Malawska, B.; Kulig, K.; Spiewak, A.; Stables, J. P. *Bioorg. Med. Chem.* **2004**, *12*, 625.
18. Tasso, S. M.; Moon, S. Y.; Bruno-Blanch, L. E.; Estiú, G. L. *Bioorg. Med. Chem.* **2004**, *12*, 3857.
19. Estrada, E.; Peña, A. *Bioorg. Med. Chem.* **2000**, *8*, 2755.
20. Bäckbro, K.; Lowgren, S.; Osterlund, K.; Atepo, J.; Unge, T.; Hulten, J.; Bonham, N. M.; Schaal, W.; Hallberg, A. *J. Med. Chem.* **1997**, *40*, 898.
21. Hulten, J.; Bonham, N. M.; Nillroth, U.; Hansson, T.; Zuccarello, G.; Bouzide, A.; Aqvist, J.; Classon, B.; Danielson, U. H.; Karlen, A.; Kvarnstrom, I.; Samuelsson, B.; Hallberg, A. *J. Med. Chem.* **1997**, *40*, 885.
22. Castro, J. L.; Baker, R.; Giublin, A. R.; Hobbs, S. C.; Jenkins, M. R.; Rusell, M. G. N.; Beer, M. S.; Stanton, J. A.; Scholey, K.; Hargreaves, R. J. *J. Med. Chem.* **1994**, *37*, 3023.
23. Acheson, R. M.; Bite, M. G.; Kemp, J. E. G. *J. Med. Chem.* **1981**, *24*, 1300.
24. Dougherty, J. M.; Probs, D. A.; Robinson, R. E.; Moore, J. D.; Klein, T. A.; Snelgrove, K. A.; Hanson, P. R. *Tetrahedron* **2000**, *56*, 9781.
25. Abbate, F.; Supuran, C. T.; Scozzafava, A.; Orioli, P.; Stubbs, M. T.; Klebe, G. *J. Med. Chem.* **2002**, *45*, 3583.
26. Winum, J.-Y.; Innocenti, A.; Nasr, J.; Montero, J.-L.; Scozzafava, A.; Vullo, D.; Supuran, C. T. *Bioorg. Med. Chem. Lett.* **2005**, *15*, 2353.
27. Casini, A.; Winum, J.-Y.; Montero, J.-L.; Scozzafava, A.; Supuran, C. T. *Bioorg. Med. Chem. Lett.* **2003**, *13*, 837.
28. Winum, J.-Y.; Cecchi, A.; Montero, J.-L.; Innocenti, A.; Scozzafava, A.; Supuran, C. T. *Bioorg. Med. Chem. Lett.* **2005**, *15*, 3302.
29. Maryanoff, B. E.; McComsey, D. F.; Costanzo, M. J.; Hochman, C.; Smith-Swintosky, V.; Shank, R. P. *J. Med. Chem.* **2005**, *48*, 1941.
30. Supuran, C. T.; Scozzafava, A. *Expert Opin. Ther. Pat.* **2000**, *10*, 575.
31. Supuran, C. T.; Scozzafava, A. *Curr. Med. Chem.: Immune. Endocr. Metab. Agents* **2001**, *1*, 61.
32. Shank, R. P.; Gardocki, J. F.; Streeter, A. J.; Maryanoff, B. E. *Epilepsia* **2000**, *41*(Suppl. 1), S3.
33. Shank, R. P.; Gardocki, J. F.; Vaught, J. L.; Davis, C. B.; Schupsky, J. J.; Raffa, R. B.; Dodgson, S. J.; Nortey, S. O.; Maryanoff, B. E. *Epilepsia* **1994**, *35*, 450.
34. SYBYL 6.6; Tripos Inc., 1699 South Hanley Rd., St. Louis, MO 63144, USA.
35. White, H. S. *Epilepsia* **1999**, *40*(Suppl. 5), S2.
36. Pugsley, M. K.; Yu, E. J.; Mc.Lean, T. H.; Goldin, A. L. *Proc. West. Pharmacol. Soc.* **1999**, *42*, 105.
37. Chufan, E. E.; Pedregosa, J. C.; Baldini, O. N.; Bruno Blanch, L. E. *Il Farmaco* **1999**, *54*, 838.
38. Tasso, S. M.; Bruno-Blanch, L. E.; Moon, S. Y.; Estiú, G. L. *J. Mol. Struct. (Theochem)* **2000**, *504*, 229.
39. Frisch, M. J.; Trucks, G. W.; Schlegel, H. B.; Scuseria, G. E.; Robb, M. A.; Cheeseman, J. R.; Zakrzewski, V. G.;

Montgomery, J. A. Jr.; Stratmann, R. E.; Burant, J. C.; Dapprich, S.; Millam, J. M.; Daniels, A. D.; Kudin, K. N.; Strain, M. C.; Farkas, O.; Tomasi, J.; Barone, V.; Cossi, M.; Cammi, R.; Mennucci, B.; Pomelli, C.; Adamo, C.; Clifford, S.; Ochterski, J.; Petersson, G. A.; Ayala, P. Y.; Cui, Q.; Morokuma, K.; Malick, D. K.; Rabuck, A. D.; Raghavachari, K.; Foresman, J. B.; Cioslowski, J.; Ortiz, J. V.; Baboul, A. G.; Stefanov, B. B.; Liu, G.; Liashenko, A.; Piskorz, P.; Komaromi, I.; Gomperts, R.; Martin, R. L.; Fox, D. J.; Keith, T.; Al-Laham, M. A.; Peng, C. Y.; Nanayakkara, A.; Challacombe, M.; Gill, P. M. W.; Johnson, B.; Chen, W.; Wong, M. W.; Andres, J. L.; Gonzalez, C.; Head-Gordon, M.; Replogle, E. S.; Pople, J. A. **1998**, Gaussian 98, Revision A.9 Gaussian Inc., Pittsburgh PA.

40. Bermann, M.; Van Wazer, J. R. *Synthesis* **1972**, *10*, 576.
41. Gong, B.; Zheng, C.; Skrzpczak-Jankun, E.; Yan, Y.; Zhang, J. *J. Am. Chem. Soc.* **1998**, *120*, 11194.
42. Gong, B.; Zheng, C.; Skrzypczak-Jankun, E.; Yan, Y.; Zhang, J. *J. Am. Chem. Soc.* **1999**, *121*, 9766.
43. Vandi, A.; Moeller, T.; Audrieth, L. F. *J. Org. Chem.* **1961**, *26*, 1136.
44. Sowada, V. R. *J. Prakt. Chem.* **1963**, *4*, 310.
45. Ohme, R.; Preuschhof, H. *Liebigs Ann. Chem.* **1968**, *713*, 74.
46. Gavernet, L.; Saraví Cisneros, H.; Bruno-Blanch, L. E.; Estiú, G. L. *Theor. Chem. Acc.* **2003**, *110*, 434.
47. Fisher, R. S. *Brain Res. Rev.* **1989**, *14*, 245–278.
48. Gladding, G. D.; Kupferberg, H. J.; Swinyard, E. A. In *Handbook of Experimental Pharmacology*; Frey, H., Janz, D., Eds.; Springer: Berlin, 1985; pp 341–347.
49. Rogawski, M.; Porter, R. *Pharmacol. Rev.* **1990**, *49*, 223.
50. Porter, M.; Cereghino, M.; Gladding, R.; Hessie, B.; Kupferberg, D.; Scoville, M.; White, D. *Cleveland Clin. Q.* **1984**, *51*, 293.
51. Molnar, P.; Erdo, S. L. *Eur. J. Pharmacol.* **1995**, *273*, 303.
52. Maryanoff, B.; Costanzo, M.; Nortey, S.; Greco, M.; Shank, R.; Schupsky, J.; Ortegon, M.; Vaught, J. *J. Med. Chem.* **1998**, *41*, 1315.
53. Grimm, H. G. *Z. Electrochem.* **1925**, *31*, 474.
54. Grimm, H. G. *Z. Naturwissenschaften* **1929**, *17*, 557.
55. Patani, G. A.; LaVoie, E. J. *Chem. Rev.* **1996**, *96*, 3147.
56. Litchfield, J. T.; Wilcoxon, F. *J. Pharmacol. Exp. Ther.* **1949**, *96*, 99.